Surface Science 685 (2019) 19–23

Contents lists available at ScienceDirect

Surface Science

journal homepage: www.elsevier.com/locate/susc

Superstructures of Se adsorbates on Au(111): Scanning tunneling microscopy and spectroscopy study

Minjun Lee[a], Sungmo Kang[a], Myungchul Oh[a], Jungseok Chae[b,c,*], Jaejun Yu[a], Young Kuk[a,b,*]

[a] Department of Physics and Astronomy, Seoul National University, Seoul 08826, Republic of Korea
[b] Center for Quantum Nanoscience, Institute for Basic Science, Seoul 03760, Republic of Korea
[c] Department of Physics, Ewha Womans University, Seoul 03760, Republic of Korea

ARTICLE INFO

Keywords:
Selenium film
Quantum bound states
Surface state

ABSTRACT

We studied the geometric and local electronic structure of a Se-adsorbed Au(111) surface. The reconstructed herringbone structure disappeared and the Au(111) surface states were attenuated with Se adsorption on the Au (111) surface, as explained by density functional theory calculations. Electron interference patterns were observed on the exposed Au (111) surface due to electron scattering by potential barriers formed by Se adsorbates. A strong bound state from the Se *p*-orbital on top of the Se clusters with quantum confinement effects were observed using scanning tunneling microscopy and spectroscopy.

1. Introduction

The electronic structures of very thin metal or metalloid films on metal surfaces have attracted attention because of their quantum mechanical bound-state effects [1–4]. In the presence of a thin film, the surface states of the substrate metal and the electronic structure of the thin film differ significantly from that of the bulk. For metallic films, the quantum mechanical bound-state effect is easily predicted, but with metalloids, it is difficult because of the relatively strong chemical bonds between the film and substrate atoms. A clean Au(111) surface reveals a well-known (23 × √3)-reconstructed herringbone structure [5]. The surface shows a surface state at −450 meV [6]; similar surface states have also been found on other noble metals such as Cu(111) and Ag (111) by photoemission spectroscopy [7] and scanning tunneling spectroscopy (STS) [8]. These surface states induce several surface phenomena such as Friedel oscillation [9] and quantum confinement [10], which are still being studied [11]. Typical metalloid films comprising chalcogenides, such as Se or Te form strong chemical bonds with metal substrates, yielding unique electrical properties in the film. These phenomena are also evident in recently reported results of adsorbate-induced bound states observed using scanning tunneling microscopy (STM) and STS [4]. Here, we report the geometric and electronic structures of a Se-adsorbed Au(111) surface. We have observed that Se atoms self-assemble as (√3 × √3)R30° Se superstructures, such as linear chains and triangular islands. We resolve the atomic structures and local electronic states on top of Se superstructures and the exposed Au (111) surface near Se superstructures using STM and STS.

2. Methods

2.1. Sample preparation

Before depositing Se on an Au(111) surface, a clean Au(111) surface was prepared by two or three cycles of Ar sputtering for approximately 20 min and annealing at 450 °C for approximately 1 h in an ultrahigh vacuum (UHV) chamber. Then the Au(111) surface was then exposed to Se atomic gas to form Se superstructures. Se of 99.999% high-purity (Alfa Aesar) was evaporated using a home-made, Knudsen cell and the evaporation rate was calibrated by a thickness monitor. An Au(111) single crystal of a high purity of 99.999% (MaTeck) was used.

2.2. STM experiments

We used a home-built STM with a sample preparation chamber (base pressure of 1×10^{-10} Torr). The *dI/dV* spectra and *dI/dV* maps were obtained by using the lock-in technique as opening the feedback loop and applying a modulation of 211 Hz with the amplitude of several millivolts. An Ir tip (Alfa Aesar, 99.999%) was prepared by electrochemical etching, followed by sharpening using a focused ion beam (FIB) and cleaning by e-beam heating in a UHV preparation chamber. All STM experiments were performed at 4.3 K.

* Corresponding authors at: Center for Quantum Nanoscience, Institute for Basic Science, Seoul 03760, Republic of Korea.
E-mail addresses: chae.jungseok@qns.science (J. Chae), ykuk@phya.snu.ac.kr (Y. Kuk).

https://doi.org/10.1016/j.susc.2019.03.002
Received 11 January 2019; Received in revised form 26 February 2019; Accepted 3 March 2019
Available online 04 March 2019
0039-6028/

2.3. Density functional theory calculation

Electronic structure calculations using density functional theory (DFT) were performed using the Vienna *Ab initio* Simulation Package (VASP) [12]. The generalized gradient approximation (GGA) functional in the Perdew, Burke and Enzerhof parameterization was used [13]. For detailed parameters, we used the energy cutoff of 500 eV, energy criterion of 1.0×10^{-6} eV, force criterion of 0.005 eV/Å, and K-point grids of $11 \times 11 \times 1$ for the layered structure. In the unit cell, there was almost 30 Å of vacuum. We used Bandup code to obtain the unfolded band structure. In the calculations, we first performed an electronic structure calculation for the Se-adsorbed Au(111) structure corresponding to the $(\sqrt{3} \times \sqrt{3})R30^{\circ}$ superstructure. Band unfolding from the superstructure to the primitive unit cell was performed for comparison with calculation results of the pure Au(111) layered-structure.

2.4. MATLAB simulation

Electron interference patterns on exposed Au(111) surface with submonolayer covered Se were simulated using MATLAB. The atomic position of each Se atom was obtained from STM topographic images to demonstrate the electron interference patterns. All Se atoms were defined as 4.4 Å in size and isotropic scattering centers. The phase information was set to change by 180° with each scattering incident.

3. Results and discussion

Fig. 1(a) presents STM topographic images of Se clusters on the Au (111) surface, which form $(\sqrt{3} \times \sqrt{3})R30^{\circ}$ structures, similar to those in Te adsorbed Au(111) surface [4]. Each Se cluster includes some regular structures such as atomic chains and triangular islands. Fig. 1(b) shows a partially exposed Au(111) herringbone structure far from Se clusters. However, the herringbone structure disappears near Se clusters. Fig. 1(c) presents the DFT calculation for the relation between the energy minimum and interatomic distance. The interatomic distance of bulk Au(111) is 2.95 Å at the energy minimum from geometric relaxation. However, an isolated Au monolayer has an energy minimum with the interatomic distance of 2.75 Å. The topmost layer of Au(111) experiences compressive force from this reduced interatomic distance, characteristic of top-most layer on the Au(111). This is because one side of the layer is terminated by vacuum, while the other side is in contact with bulk Au(111), which provides the holding force to maintain the interatomic distance of bulk Au(111). In the presence of buckled herringbone boundaries, repeated hexagonal-close-packed (hcp) stacking and face-centered-cubic (fcc) stacking are low-energy configuration on a clean Au(111). However, as the Se atoms are adsorbed on the surface, as shown in Fig. 1(c), the compressive force is relaxed, resulting that the fcc stacking is a lower energy configuration. Therefore, no herringbone structure is observed near the Se clusters.

Fig. 2(a) shows a high-resolution topographic image of Se clusters on an Au(111) surface. We measured the local density of states (LDOS) on the exposed Au(111) surface and on one Se cluster by STM-STS. Fig. 2(b) presents tunneling spectra of the exposed Au(111) surface and the Se cluster. On the clean Au(111) surface, STM-STS typically show a strong surface state approximately at −450 mV [6]. On Se adsorbed Au (111), we observed a weak surface state approximately at −466 meV. The Se atoms act as impurities on the Au(111) surface, the surface state is weaker than on a clean Au(111) surface. In addition to this weak surface state, relatively regular peaks occur above the energy of the surface state. Using Gaussian fitting, we locate the peak centers at −74, 114, 302, 459, 655, and 881 meV. From this LDOS, it is estimated that we measured the quantum confinement state of electrons on the Au (111) surface enclosed by potential barriers of Se adsorbates. The surface electrons are localized on the surface because of the blockage by a vacuum gap on one side and by the *sp*- band gap of bulk Au (111) on the other side. Therefore, surface electrons can be treated as quasi-2D free

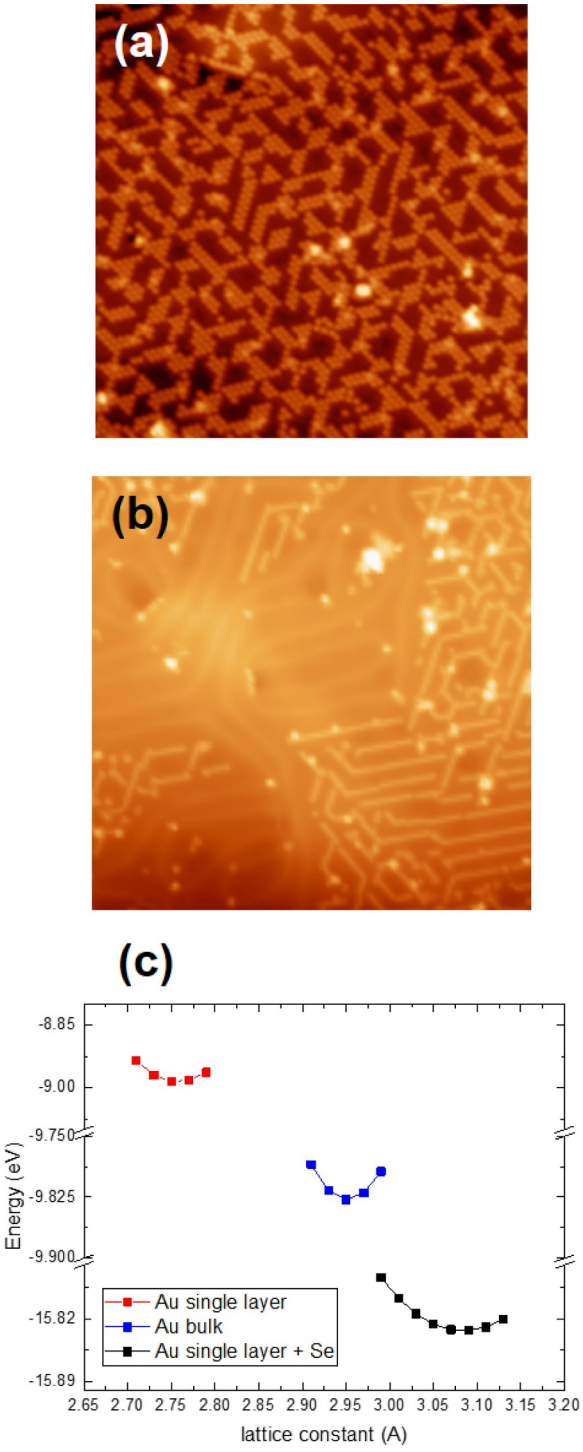

Fig. 1. STM topographies and calculations for Se on Au(111) and the disappearance of herringbone structure. (a) Regularly embedded Se adatoms on Au(111) (tunneling current I_t = 100 pA; bias voltage V_b = 1 V; 30 × 30 nm) (b) disappearance of herringbone structures by Se adatoms (I_t = 10 pA; V_b = −3 V; 105 × 105 nm) (c) Calculation of interatomic distance with energy minimization of Au single layer (red curve), bulk Au (blue curve) and fully Se-covered Au single layer (black curve).

electrons. In addition, the potential barrier by Se adsorbates confines the quasi 2D free-electrons, yielding quantum confinement states. Fig. 2(b) also presents tunneling spectrum on the Se cluster. It has a strong localized state at approximately −607 meV, which corresponds to the Se 4*p*- orbital state from the DFT calculation. Fig. 2(c) shows the DFT-calculated band structure of this system including the pure Au

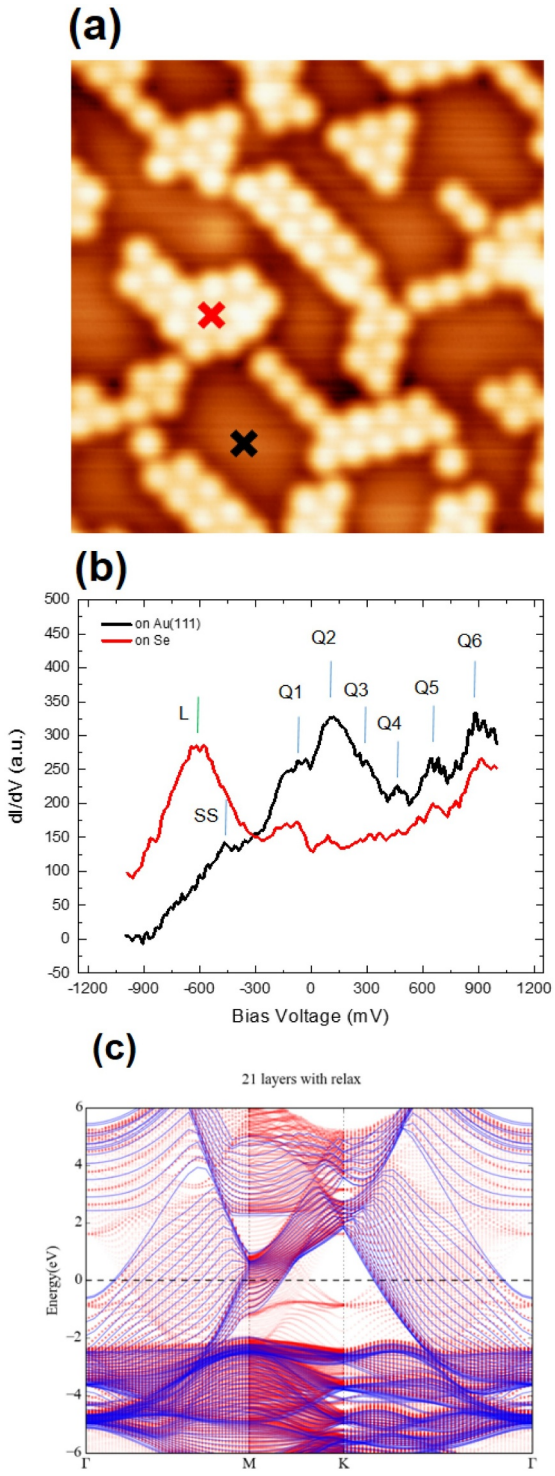

Fig. 2. Tunneling spectra and band structure of Se on Au(111). (a) Close-up image of Se clusters on Au(111) (I_t = 50 pA; V_b = 200 mV; 8 × 8 nm) (b) Tunneling spectrum on exposed Au(111) surface at the black cross on Fig. 2(a). STM spectrum of a Se cluster at the red cross on Fig. 2(a). (SS: surface state, Qs: Quantum bound states, L: Localized state of Se). (c) Band structures of Au(111) (blue curves) and Se-covered Au(111) (red curves).

(111) band structure and the unfolded band structure for the fully Se-covered Au(111) system. A flat band derived from the 4*p* orbital of Se is formed between the M point and the K point near -600 meV on the Se-covered Au(111) surface, which is consistent with our measurements.

Fig. 3(a)–(d) show the LDOS maps of Se clusters on the Au(111) surface at the energies of −1200, −550, 100, and 200 meV, respectively. Electron interference patterns appear on the exposed Au(111) surface at 100 and 200 meV, above the energy of the surface state of Au (111). Otherwise, no interference patterns appear at −1200, −550 meV, below the energy of the Au surface state. This is because the quai-2D free electrons only exist on the Au(111) surface above the minimum energy of the surface state dispersion at −466 meV, which interfere with each other to yield interference patterns. Every Se adatoms appears as a dark dot, indicating that they act as scattering centers for quasi-2D free electrons on the Au(111) surface. To analyze the diffraction patterns, we assumed that the Au surface electrons act as nearly free- electrons. We simulated the interference patterns (Fig. 3(e, f)) with the wavelengths of 2.38 nm and 2.15 nm. These values almost match the experimental result. From the parabolic dispersion relation

$$E(\lambda) = E_0 + h^2/(2m^*\lambda^2) \quad (1)$$

where E_0 is the onset energy of the Au surface state. The measured band minimum of −466 meV was used for calculation of Eq. (1). A correlation function was used for comparison of the experimentally obtained images with simulated ones to extract the value of wavelength. After several simulations we made a plot of the correlation function versus wavelength, and determined the optimal value of the wavelength to maximize the correlation function by the Lorentzian fitting. With a parabolic fitting with data points, m^* is thus determines as 0.48 ± 0.02 m_e. The Shockley state electrons on a clean Au(111) has the effective mass of 0.28 m_e in the topmost plane of a clean [14] and that can be confirmed in Shockley s-electron dispersion (blue line) along the Γ direction in our DFT calculation in Fig. 2c. In the presence of Se adsorbates, the Shockley s-electron dispersion (red line) flatten substantially on exposed Au surface around Se adsorbates as shown in our calculation (Fig. 2c). The surface state electron is still nearly free-electron but with heavier mass with Se adsorbates. Fig. 4(a) depicts the topographic image of a diamond-shaped Se-cluster on the Au(111) surface. On this regularly shaped cluster, we performed *dI/dV* maps at various bias voltages of −1600 meV, −1100 meV, −550 meV, −200 meV, and +1000 meV (Fig. 4(b)–(f)), respectively. The electron density on the diamond Se cluster forms quantum confinement states. At −1600 meV, the interior of the Se cluster is dark, indicating the low and homogeneous electron density inside the Se cluster. However, at −1100 meV, the center of the Se cluster is darker than the edge. This situation is reversed at −550 meV, so that the electron density at the center of the cluster is larger than that at the edge. These kinds of patterns are changed with the mapping energy, a well-known phenomenon of quantum confinement states [15–17].

In summary, we observed the Se-adsorbed Au(111) surface using STM. Se adsorption removes the original Au herringbone structure and reduces the surface state energy. Se clusters have strong localized states, which show good agreement with DFT calculations. On the Se adsorbed Au(111) surface, Se atoms act as energy barriers and scattering centers, that yields electron interference patterns around them. In addition, the Se atomic clusters itself forms quantum confinement states within the cluster and shows energy-dependent interference patterns. This system is a good template to study quasi-2D free- electrons and their interference phenomena.

Acknowledgments

This work is supported in part by the National Research Foundation of Korea (NRF) Grant (NRF-2010-00349). JC is supported by the IBS research program IBS-R027-D1.

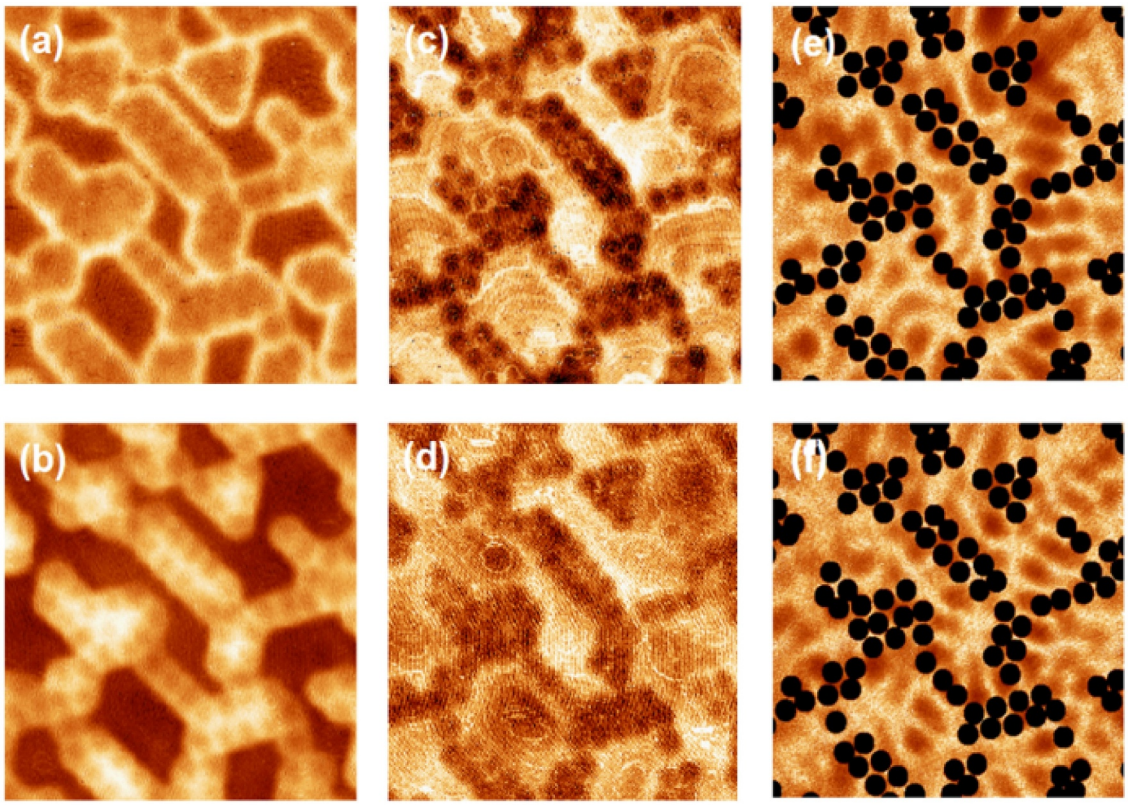

Fig. 3. LDOS maps of Se on Au(111) from STM dI/dV images. (a)–(d) LDOS maps for −1200 mV, −550 mV, 100 mV, and 200 mV (8 × 8 nm^2). Every map taken by tunneling current of 100 pA and modulation voltage of 5 mV. (e) and (f) MATLAB simulation of LDOS map for 100 meV and 200 meV, respectively.

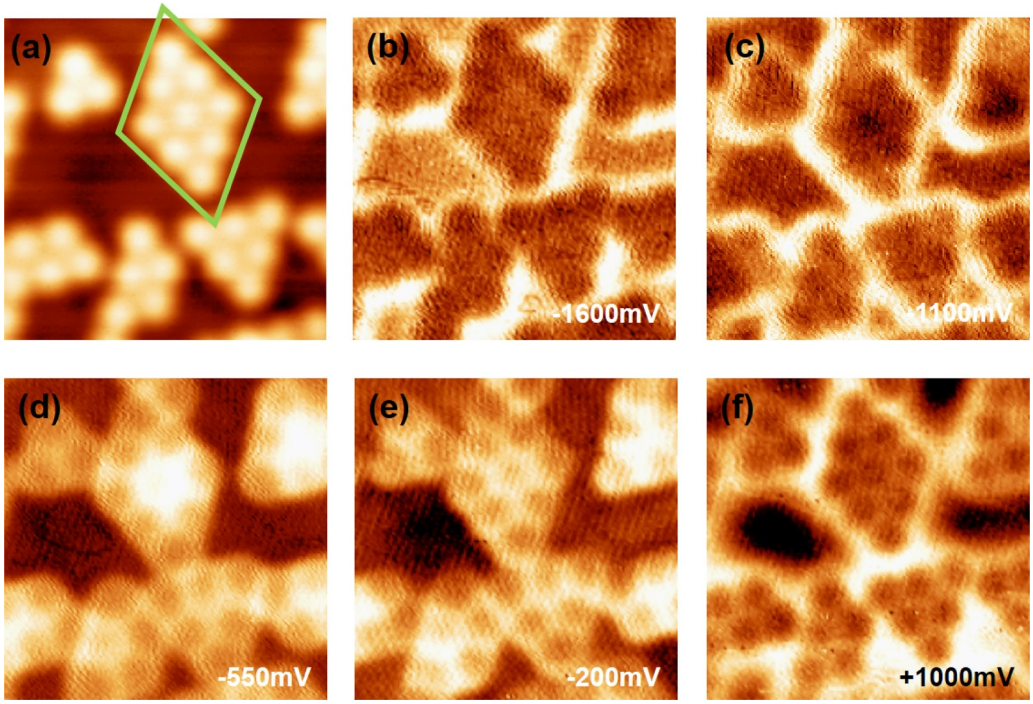

Fig. 4. Localized states of Se on Au(111). (a) STM topography of Se clusters (I_t = 50 pA; V_b = 1 V; 4.5 × 4.5 nm^2). (b)–(f) dI/dV map of Se clusters at the same area of Fig. 4(a) with bias voltage of −1600 mV, −1100 mV, −550 mV, −200 mV and +1000 mV, respectively.

Supplementary materials

Supplementary material associated with this article can be found, in the online version, at doi:10.1016/j.susc.2019.03.002.

References

[1] T.E. Lister, J.L. Stickney, J. Phys. Chem. 100 (1996) 19568.
[2] L. Gao, J.-T. Sun, J.-C. Lu, H. Li, K. Qian, S. Zhang, Y.-Y. Zhang, T. Qian, H. Ding, X. Lin, S. Du, H.-J. Gao, Adv. Mater. 30 (2018) 1707055.
[3] X. Lin, J.C. Lu, Y. Shao, Y.Y. Zhang, X. Wu, J.B. Pan, L. Gao, S.Y. Zhu, K. Qian, Y.F. Zhang, D.L. Bao, L.F. Li, Y.Q. Wang, Z.L. Liu, J.T. Sun, T. Lei, C. Liu, J.O. Wang, K. Ibrahim, D.N. Leonard, W. Zhou, H.M. Guo, Y.L. Wang, S.X. Du, S.T. Pantelides, H.-J. Gao, Nat. Mater. 16 (2017) 717.
[4] K. Schouteden, J. Debehets, D. Muzychenko, Z. Li, J.W. Seo, C.V. Haesendonck, J. Phys. 29 (2017) 125001.
[5] C. Wöll, S. Chiang, R.J. Wilson, P.H. Lippel, Phys. Rev. B 39 (1989) 7988.
[6] L.C. Davis, M.P. Everson, R.C. Jaklevic, W. Shen, Phys. Rev. B 43 (1991) 3821.
[7] S.D. Kevan, R.H. Gaylord, Phys. Rev. B 36 (1987) 5809.
[8] L. Bürgi, L. Petersen, H. Brune, K. Kern, Surf. Sci. 447 (2000) L157.
[9] L. Petersen, P. Laitenberger, E. Lægsgaard, F. Besenbacher, Phys. Rev. B 58 (1998) 7361.
[10] K. Schouteden, E. Lijnen, D.A. Muzychenko, A. Ceulemans, L.F. Chibotaru, P. Lievens, C.V. Haesendonck, Nanotechnology 20 (2009) 395401.
[11] B. Yan, B. Stadtmüller, N. Haag, S. Jakobs, J. Seidel, D. Jungkenn, S. Mathias, M. Cinchetti, M. Aeschlimann, C. Felser, Nat. Commun. 6 (2015) 10167.
[12] G. Kresse, J. Furthmüller, Phys. Rev. B 54 (1996) 11169.
[13] J.P. Perdew, K. Burke, M. Ernzerhof, Phys. Rev. Lett. 77 (1996) 3865.
[14] S.D. Kevan, R.H. Gaylord, Phys. Rev. B 36 (1987) 5809.
[15] E. Lijnen, L.F. Chibotaru, A. Ceulemans, Phys. Rev. E 77 (2008) 016702.
[16] T. Kumagai, A. Tamura, J. Phys. 20 (2008) 285220.
[17] T. Kumagai, A. Tamura, J. Phys. Soc. Jpn. 77 (2007) 014601.